OPEN ACCESS

University of Dundee

University of Dundee

Physical Modelling of Laterally Spreading Soil with and without Plant Root Analogues

Wang, Ke; Brennan, Andrew; Robinson, Scott; Knappett, Jonathan; Bengough, Glyn

Published in:
SECED 2019 Proceedings

Publication date:
2019

Document Version
Peer reviewed version

Link to publication in Discovery Research Portal

PHYSICAL MODELLING OF LATERALLY SPREADING SOIL WITH AND WITHOUT PLANT ROOT ANALOGUES

Ke WANG[1,2], Andrew BRENNAN[3], Scott ROBINSON[4], Jonathan KNAPPETT[5] & Glyn BENGOUGH[6]

Abstract: *A key problem experienced when soils liquefy during earthquakes is that gently sloping ground can translate downslope. Most recently, this lateral spreading was seen to affect large portions of coastline around Palu Bay in the 28 September 2018 Indonesia earthquake. Soil observed to experience lateral spreading frequently contains plant roots that in principle should have a reinforcing effect on the soil. However, field data is difficult to interpret due to the many uncontrollable variables, so there has not previously been an attempt to quantify roots effects on lateral spreading. Physical modelling offers an opportunity to test soil in real site conditions with controlled variables (soils, slopes, stratification etc.). In this study, a small scale model with the potential to undergo lateral spreading is created and tested on the geotechnical centrifuge. Considerations of how the model could exhibit lateral spreading without boundary interaction, and how both fibrous roots (like grass) and more woody roots (like a shrub) could be modelled in a small scale model, are discussed. The model is shown to recreate a lateral spread during centrifuge testing when the soil contains no roots. When tested in moderate-sized earthquake events, the lateral displacement was reduced by ~60% by fibrous root analogues and 70% by woody root analogues. However, in stronger events where liquefaction occurred to greater depths, then the near-surface roots offered less resistance to displacement. These results indicate that without roots, spreading could be worse, but the roots alone may not be enough to prevent damage completely, particularly in larger earthquakes.*

Introduction

Recent earthquake events such as the Indonesia earthquake, 28 September 2018, continue to show the damaging effects of soil liquefaction and associated lateral spreading. Soil observed to experience lateral spreading frequently contains plant roots. Although root reinforcement may not completely prevent an occurrence of lateral spreading, they may still contribute to limit the extent of damage which may occur in fallow ground. Therefore, it is necessary to investigate the effects of plant roots on limiting soil liquefaction-induced lateral spreading.

Using roots to increase slope stability has been widely recognized (Gray and Leiser, 1982, Coppin and Richards, 1990, Gray and Sotir, 1996) and investigations have been taken for quantifying the effects of roots (Wu, 2013), including using geotechnical centrifuge modelling involving both living plant roots (Sonnenberg et al., 2010) and 3D printed analogue root models (Liang et al., 2017). These prior studies treated roots as large structural elements, however the roots of forbs and grasses are comprised of many thin fibres, and even more substantial woody roots of shrubs or trees are connected to much finer lateral root branches. To study these, the authors previously investigated the use of artificial polypropylene fibres as model root analogues in soils, when applied to uplift of buried infrastructure in liquefiable soils (Wang et al., 2018). Using fibre-reinforcement to increase liquefaction resistance of soil was first investigated by Noorany and Uzdavines (1989) through cyclic triaxial tests, the results have been confirmed by other researchers using similar tests (e.g. Krishnaswamy and Isaac, 1994, Boominathan and Hari, 2002, Noorzad and Fardad Amini, 2014, Manafi Khajeh Pasha et al., 2016), hollow cylinder tests (Mandolini et al., 2019) and cyclic simple shear (Robinson et al., 2019). Centrifuge tests were

---

[1] Research Associate, University of Dundee, Dundee, UK, email: tonykewang@hotmail.com
[2] Engineer, Changjiang River Scientific Research Institute of Changjiang Water Resources Commission, Wuhan, China
[3] Senior Lecturer, University of Dundee, Dundee, UK, a.j.brennan@dundee.ac.uk
[4] Research Associate, University of Dundee, Dundee, UK, s.z.robinson@dundee.ac.uk
[5] Professor, University of Dundee, Dundee, UK
[6] Professor, University of Dundee & James Hutton Institute, Dundee, UK

also conducted, finding that polypropylene fibres can increase soil stiffness (Wang and Brennan, 2014) and limit significant deformation (Wang and Brennan, 2015) caused by soil liquefaction. However, all these studies either treated only a small element of soil, or incorporated fibres throughout the full liquefiable depth of soil, whereas fine fibrous roots are mainly positioned in the surface horizons.

In this study, therefore, three centrifuge tests were conducted to investigate the effects of roots systems on limiting lateral spreading caused by soil liquefaction. A benchmark test was conducted first to recreate a lateral spreading case. In the second and third tests, a fibrous roots system and a more woody roots system were respectively introduced in the near surface layer of the liquefiable backfill to represent, mechanically, plant root effects in the lateral spreading caused by soil liquefaction.

Centrifuge Modelling

Apparatus and instruments

All centrifuge tests were carried out on the Actidyn C67-2 geotechnical centrifuge under 30g (i.e. scale factor N = 30) at the University of Dundee. Input motions were excited by the Actidyn Q67-2 on board earthquake simulator, capable of applying repeatable strong motion histories to soil models (Brennan et al., 2014). Models were constructed in an equivalent shear beam container with internal dimensions of 674×312×280mm^3. This container was designed to vibrate with the same amplitude and natural frequency as sandy soil (Bertalot, 2013). Instrumentation within the models measured pore pressures and accelerations but in this paper only data from Linear variable differential transducers (LVDTs), contact transducers measuring lateral displacements and ground settlements, will be described.

Model materials

Soil models were constructed by the HST95 Congleton sand. This sand has a mean particle size D_{50}=0.13 mm, an effective size D_{10}=0.1mm, a coefficient of uniformity C_u=2.25, a coefficient of curvature C_c=1.36, a specific gravity G_s=2.63, maximum void ratio e_{max}=0.795 and minimum void ratio e_{min}=0.463.

Methylcellulose solution with 30 times viscosity of water was used as a pore fluid instead of water to overcome the disparity between the scaling laws for the time of diffusion processes and a dynamic event that would otherwise exist (Madabhushi, 2014). This means the scaling law for all time-dependent processes is $t_{prototype} = N \times t_{model}$.

The fine fibrous roots were represented by polypropylene fibres with a commercial name Lokand™ (Figure 1). They have a nominal length of 35mm and a nominal diameter of 0.1mm. Their specific gravity is 0.91, and the tensile strength is 200MPa (manufacturer values). It is acknowledged that breakage of roots may occur under high shear stresses. However, in liquefaction problems the shear stresses acting to displace the soil are similar to in-situ shear stresses and therefore root breakage is not anticipated to be a limiting mechanism. Use of fibres will enable the mechanical stiffness behaviour of rooted soil, that will govern large scale displacements, to be reproduced correctly.
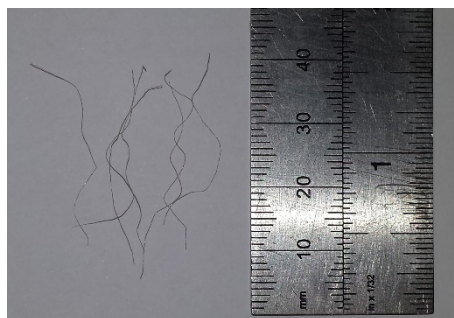

Figure 1. Loksand™ fibres (Wang et al., 2018)

The structural roots' model (Figure 2), which is part of the more woody roots system, was constructed by the uPrint SE Acrylonitrile Butadiene Styrene (ABS) prototyper (known as a 3D printer) at the University of Dundee. The detailed construction processes are described by Liang et al. (2014). The structural roots' architecture originates from the coarse roots of *Arctostaphylos*

pungens (a chaparral shrub) described by Wu et al. (2014). In order to represent the woody roots in the centrifuge model, the original root system structure provided by Wu et al. (2014) was modified (Wang et al., 2018) by increasing the diameter of the roots six times while the length remained as the original (Figure 3). This was required due to the limitations of creating small diameter ABS plastic components without breakage. The modified roots were then scaled down 30 times for the test of this study based on the centrifuge scaling laws. The maximum depth of the scaled roots' model was 20mm (0.6 m prototype).
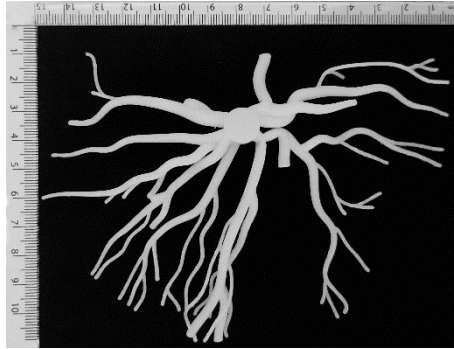

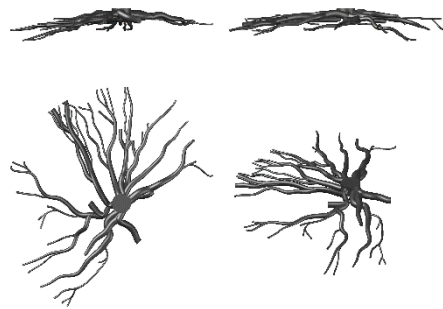*Figure 2. ABS model of woody roots, units in cm (Wang et al., 2018)*

Figure 3. Modified design of the architecture of woody roots (Wang et al., 2018)

Model profiles and test programme

The boundary value problem for producing lateral spreading in a centrifuge model is shown in Figure 4. The model consists of a stiff (non-liquefiable) layer of dense sand at the base, which slopes at an angle of 2.86° to the horizontal. This is overlain by loose sand of up to 120 mm (3.6 m prototype) depth that is intended to be potentially liquefiable. The relative densities for the loose and dense soils were 40% and 80% respectively. The loose soil is supported at one end by a wall, named the "quay wall", that rests on top of the dense substrate. On the outside of the quay wall is free water. The design is such that the quay wall balances the lateral earth pressure of the backfill under K_0 conditions, by means of friction at the base. However, when excess pore pressures are developed in the backfill during liquefaction then the backfill total earth pressure increases and exceeds the limiting friction, displacing the wall laterally until either the pore pressures reduce (i.e. the backfill pressure returns to the lower value and equilibrium is regained) or the backfill stops deforming (i.e. it becomes self-supporting and does not require a reaction force from the wall for stability). The quay wall was modelled by a watertight acrylic box with external dimensions of 140×100×267mm³. The box is filled with dry sand as ballast, its mass is 6.15kg in model scale, and the interface friction angle between the wall and the dense substrate is 17.9°. More details of the quay model can be found in the work of Wang (2018).

Three centrifuge models were included in this study. Their profiles are shown in Figure 4 and Figure 5. The first model (LS1) acted as a benchmark, representing the condition under which no mitigation method was applied. The second and third models respectively represent the conditions under which only fibrous roots (LS2) and woody roots together with fibrous roots (LS3) are applied to mitigate the lateral spreading induced by soil liquefaction. As the instrument distribution is the same in the models, it is only shown in Figure 4. Figure 6 shows the plan

distribution of woody roots' models within the backfill behind the quay wall. The dimensions shown in the figures in this section are in model scale, thus in prototype scale the fibrous roots cover the top 1.2 m soil and the woody roots extend to a depth of 0.6 m. The fibre content was 0.6% by mass or 1.2% by volume, chosen based on a maximum fraction of grass roots of 2% by volume.
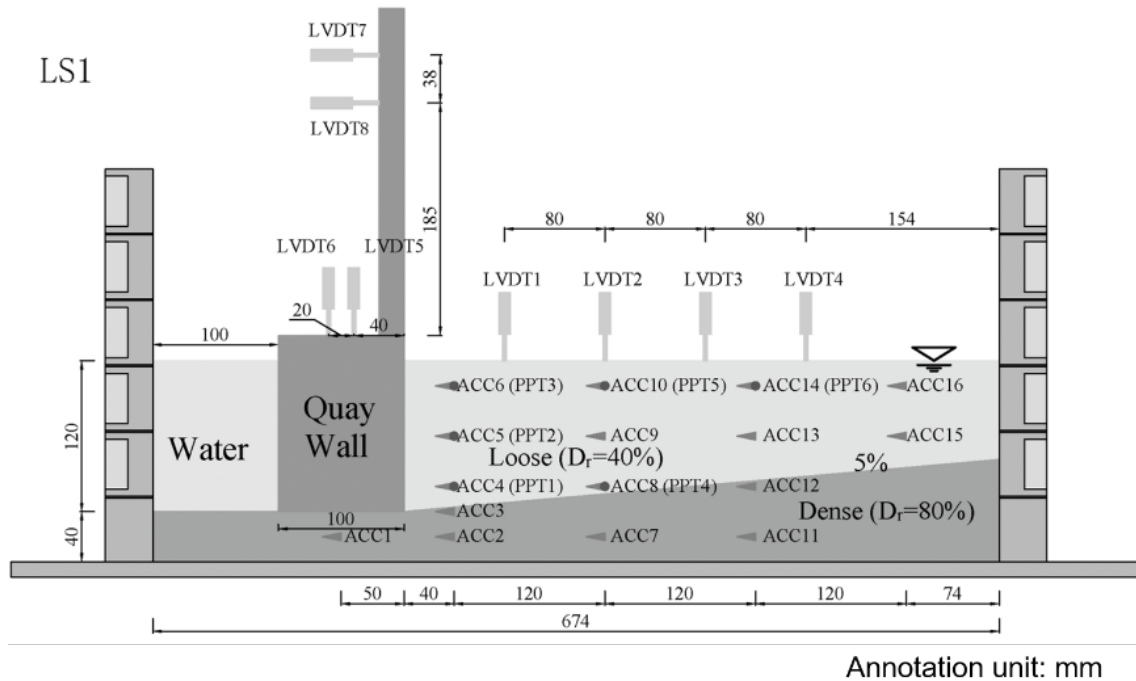

Figure 4. Centrifuge model and instrument distribution of model LS1
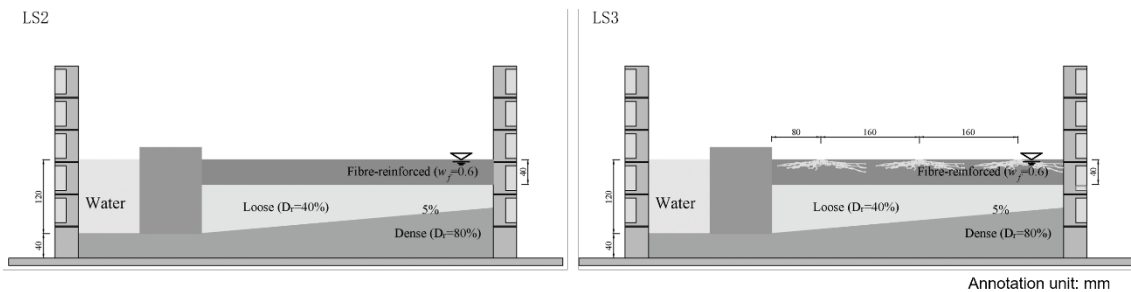
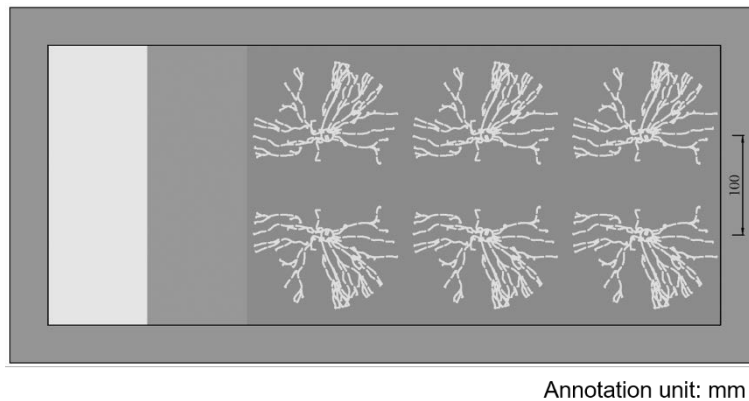

Figure 5. Schematic profiles of models LS2 and LS3

Figure 6. Plan distribution of woody roots in model LS3

After reaching the target g level of N = 30, a succession of three ground motions (EQ1, EQ2 and EQ3) were excited. There was an adequate time interval between motions to allow the completion

of movements of the quay wall and the deformation of the backfill. The ground motions are ramped sinusoidal motions with the same properties except for the maximum acceleration amplitude. The acceleration time histories of the ground motions can be described by Equation1 and plotted in Figure 7. These motions were chosen to be sinusoidal as the frequency response of the models is secondary to its liquefaction behaviour and sinusoidal motion is simpler to extract stress-strain data from accelerometers. The amplitudes and number of cycles were selected to represent three different magnitudes of event, thus the Arias intensities were taken to be comparable to real strong motion data from recent earthquakes, with examples shown for guidance in Table 1 (further details on this comparison were presented in Wang et al., 2018)

$$A(t) = \begin{cases} \dfrac{t}{nT} A_0 \sin(\omega t) & 0 \le t < nT \\ A_0 \sin(\omega t) & nT \le t < (N-n)T \\ \dfrac{NT-t}{nT} A_0 \sin(\omega t) & (N-n)T \le t \le NT \end{cases} \tag{1}$$

$$\omega = \frac{2\pi}{T} \tag{2}$$

where A=amplitude of acceleration; A_0=maximum amplitude; t=time; T=period of motion; n=number of ramped motion cycles; and N=total number of motion cycles.

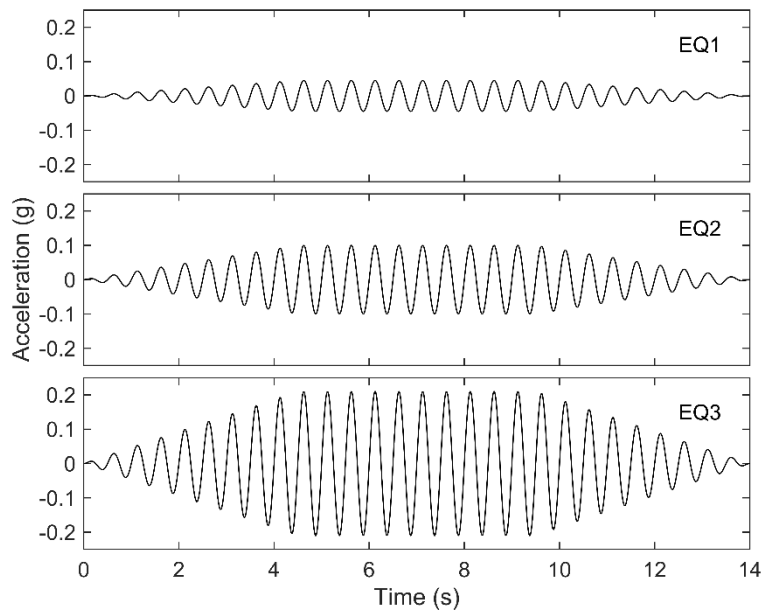| Input motion ID	A_0 (g)	T (s)	N	n	Comparable event
EQ1	0.045				Northridge earthquake, USA, 1994 (Station: Rancho Palos Verdes – Luconia, RSN 1062)
EQ2	0.100	0.5	28	9	Kocaeli earthquake, Turkey, 1999 (Station: Izmit, NGA 1165);
EQ3	0.210				Christchurch earthquake, New Zealand, 2011, (Site: Canterbury Botanical Gardens, N89W)

Table 1 Properties of ground motions (prototype scale)

Figure 7. Time histories of ground motions

Test results

Lateral displacements of the quay wall

An indication of seismic displacement during lateral spreading, the time histories of the lateral displacements of the quay wall in prototype scale are compared in Figure 8. These displacements are derived from the average of the measurements of LVDT7 and LVDT8 which, as shown in Figure 4, indicate lateral displacement (average value) and rotation (difference – which was negligible and not shown) of the wall. The lateral displacements mainly occurred co-seismically, and they increase with the rising intensities of the ground motions. It can also be seen that the lateral displacement in each ground motion event was much less in the presence of the root systems especially the one with both fibrous and structural roots in LS3. The relative lateral displacement is the one occurred in a specific ground motion event. The relative displacements for each earthquake individually are tabulated in Table 2. Also in Table 2, the displacement in the rooted tests is expressed as a proportion of the equivalent unrooted tests LS1. In each test, the displacement induced by strong EQ3 ground motion accounted for more than 55% of the accumulated displacement. The ultimate accumulative lateral displacement after three ground motions was reduced from 409mm in LS1 to 345mm in LS2 and 274 in LS3. In other words, around 15% accumulative displacement was reduced by the fibrous roots system, and around 30% was reduced by the woody-rooted system. The structural roots themselves contribute 15% to the displacement reduction. However, as shown in the breakdown in Table 2, concentrated much stronger reinforcing effect was observed during the lower magnitude event EQ1 where displacements were strongly limited. In stronger motions, although some reinforcement occurred, much less benefit was felt as a result of the presence of either root system, though in the woody case (LS3), the reinforcement in EQ3 is still broadly reflective of the cumulative effect (24% and 30%, respectively). The reduction in reinforcing effect compared to EQ1, particularly for LS2 (fibrous roots only), is attributed to soil liquefaction occurring to a greater depth in the backfill during these stronger earthquakes, and consequently the stronger surface layer may be readily transported by the liquefied substrata.
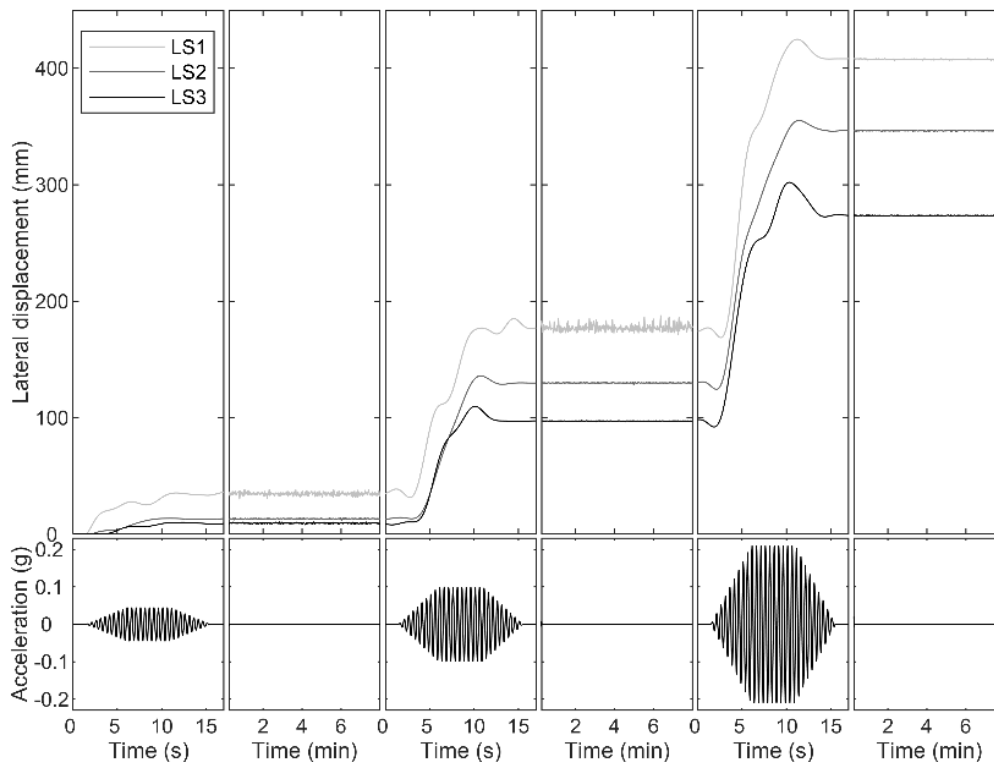

Figure 8. Time histories of accumulative lateral displacements. LS1: no roots, LS2: fibrous roots, LS3: woody and fibrous roots.

6

Input motion	LS1	LS2		LS3	
	Displacement	Displacement	% reduction	Displacement	% reduction
EQ1	35 mm	13 mm	62.8%	10 mm	71.4%
EQ2	141mm	116 mm	17.7%	88 mm	37.6%
EQ3	233 mm	216 mm	7.3%	176 mm	24.4%

Table 2. Lateral displacement and percentage reduction in accumulated displacement per earthquake for the three centrifuge models

Ground settlements of the backfill

Lateral displacements of the quay wall away from the backfill creates greater volume behind it, resulting in ground settlements of the backfill. The backfill also settles because of soil consolidation caused by post-shaking pore pressure dissipation (as in level ground). Therefore, the measured ground settlements are the joint results from these two factors. The time histories of ground settlements of backfill measured LVDT1 are shown in Figure 9, in prototype scale.
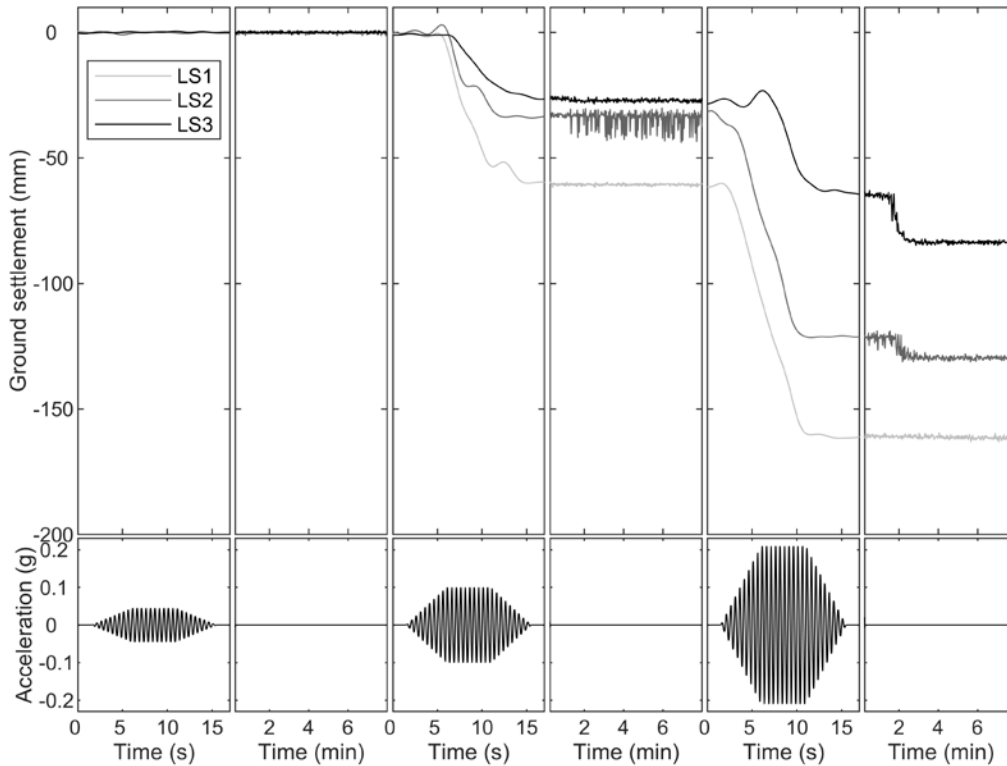

Figure 9. Time histories of ground settlements. LS1: no roots, LS2: fibrous roots, LS3: woody and fibrous roots.

Input motion	LS1	LS2		LS3	
	Displacement	Displacement	% reduction	Displacement	% reduction
EQ1	0 mm	0 mm	0%	0 mm	0%
EQ2	60mm	32 mm	46.7%	26 mm	56.7%
EQ3	100 mm	98 mm	2.0%	58 mm	42.0%

Table 3. Vertical settlements behind wall (position 2.4 m behind wall) per earthquake

The ground settlements were also reduced by the introduction of root systems as a mitigation method. The relative ground settlement is the settlement in a specific ground motion event. Table 3 presents the settlements for each earthquake. In EQ1 event, there are little settlements in three models. The main reasons for such small displacements might be that: (1) EQ1 ground motion was too gentle to induce deep soil liquefaction in the backfill; (2) lateral displacement of the quay wall – although nonzero (see above) - was too small to cause obvious settlement of the backfill; (3) the sensitivity of LVDTs is not high enough to detect such small settlement. As the ground settlements in LS1 and LS2 for the EQ3 event were similar, it suggests that the fibrous roots may lose their function for reducing ground settlements in intensive ground motions. As with the lateral displacement measurements, this data shows that the roots are more beneficial when shaking is less intense. It also shows that the larger woody roots do have a significant benefit above what fibres alone can offer. This benefit is still apparent for the strongest of the three earthquakes, suggesting that shrubs with woody roots will offer greater resilience to lateral spreading than fibrous roots alone.

Conclusions

This study described centrifuge modelling of woody and fibrous roots in limiting lateral spreading caused by soil liquefaction of the backfill behind a quay wall. Both root analogue systems reduced lateral displacements caused by the liquefaction of the backfill at various intensity levels of ground motions. The lateral displacement during a moderate earthquake event was reduced by 63% for the fibrous roots system and 71% for the more woody root system. In stronger earthquakes this effect was less marked, likely due to deeper liquefaction. The ground settlements of the backfill was also reduced by introducing root system in the top layer of the backfill. Fibrous root systems may lose their function in intensive ground motions while the more woody root systems are still effective. The vertical settlement behind the wall showed a similar pattern, suggesting that shrub-like plants show some promise in resisting lateral spreading.

Although using roots systems cannot completely prevent the damage caused by lateral spreading, it is still promising as a low-cost method to reduce the extent to which damage would occur without applying any mitigation method, especially in areas of moderate seismicity where large earthquakes are unlikely and where the cost of more extensive engineered reinforcement methods cannot be justified. Furthermore, when field data is interpreted, the likely depth of liquefaction should be compared to the depth of vegetative rooting to assess whether lateral spreading was decreased by the presence of roots.

Acknowledgement

References

Bertalot D (2013), Seismic behaviour of shallow foundations on layered liquefiable soils, PhD Thesis, University of Dundee, Dundee, UK.

Boominathan A and Hari S (2002), Liquefaction strength of fly ash reinforced with randomly distributed fibers, Soil Dynamics and Earthquake Engineering, 22(9)**:** 1027-1033.

Brennan AJ, Knappett JA, Bertalot D, Loli M, Anastasopoulos I and Brown MJ (2014), Dynamic centrifuge modelling facilities at the University of Dundee and their application to studying seismic case histories, Gaudin, C and White D (eds.), Physical Modelling in Geotechnics - Proceedings of the 8th International Conference on Physical Modelling in Geotechnics 2014, ICPMG 2014, Perth Australia, 14-17 January 2014.

Coppin NJ and Richards IG (1990), Use of vegetation in civil engineering, London: Construction Industry Research and Information Association London.

Gray DH and Leiser AT (1982), Biotechnical slope protection and erosion control, New York: Van Nostrand Reinhold Company Inc.

Gray DH and Sotir RB (1996), Biotechnical and soil bioengineering slope stabilization: a practical guide for erosion control, Hoboken: John Wiley & Sons.

Krishnaswamy N and Isaac NT (1994), Liquefaction potential of reinforced sand, Geotextiles and Geomembranes, 13(1)**:** 23-41.

Liang, T., Knappett, J.A., Bengough, A.G. & Ke, Y.X. (2017). Small scale modelling of plant root systems using 3-D printing, with applications to centrifuge modelling of root-reinforced slopes. Landslides, 14: 1747-1765. Liang T, Knappett JA and Bengough AG (2014), Scale modelling of plant root systems using 3-D printing, Gaudin, C and White D (eds.), Physical Modelling in Geotechnics - Proceedings of the 8th International Conference on Physical Modelling in Geotechnics 2014, ICPMG 2014, Perth, Australia 14-17 January 2014.

Madabhushi G (2014), Centrifuge modelling for civil engineers, Boca Raton: CRC Press.

Manafi Khajeh Pasha S, Hazarika H, Bahadori H and Chaudhary B (2016), Dynamic behaviour of saturated sandy soil reinforced with non-woven polypropylene fibre, International Journal of Geotechnical Engineering**:** 1-12.

Mandolini A, Diambra A and Ibraim E (2019) Strength anisotropy of fibre reinforced sands under multiaxial loading. Geotechnique, 69(3): 203-216.

Noorany I and Uzdavines M (1989), Dynamic behavior of saturated sand reinforced with geosynthetic fabrics, Proceedings of Geosynthetics '89, San Diego USA, 21-23 February 1989.

Noorzad R and Fardad Amini P (2014), Liquefaction resistance of Babolsar sand reinforced with randomly distributed fibers under cyclic loading, Soil Dynamics and Earthquake Engineering, 66**:** 281-292.

Robinson S, Brennan AJ, Knappett JA, Wang K and Bengough AG (2019), Cyclic simple shear testing for assessing liquefaction mitigation by fibre reinforcement, Proceedings of 7th International Conference on Earthquake Geotechnical Engineering. In press.

Sonnenberg R, Bransby MF, Hallett PD, Bengough AG, Mickovski SB and Davies MCR (2010), Centrifuge modelling of soil slopes reinforced with vegetation, Canadian Geotechnical Journal, 47(12)**:** 1415-1430.

Wang K (2018), Evaluation of fibre-reinforcement as a mitigation method against earthquake induced liquefaction hazards by centrifuge modelling, University of Dundee, Dundee, UK.

Wang K and Brennan AJ (2014), Centrifuge modelling of saturated fibre-reinforced sand, Gaudin, C and White D (eds.), Physical Modelling in Geotechnics - Proceedings of the 8th International Conference on Physical Modelling in Geotechnics 2014, ICPMG 2014, Perth, Australia, 14-17 January 2014.

Wang K and Brennan AJ (2015), Centrifuge modelling of fibre-reinforcement as a liquefaction countermeasure for quay wall backfill, 6th International Conference on Earthquake Geotechnical Engineering, Christchurch, New Zealand, 1-4 November 2015.

Wang K, Brennan AJ, Knappett JA, Robinson S and Bengough AG (2018), Centrifuge modelling of remediation of liquefaction-induced pipeline uplift using model root systems, Mcnamara, A, Divall S and Goodey R (eds.), Physical Modelling in Geotechnics - Proceedings of the 9th International Conference on Physical Modelling in Geotechnics 2018, ICPMG 2018, London, UK,

Wu TH (2013), Root reinforcement of soil: review of analytical models, test results, and applications to design, Canadian Geotechnical Journal, 50(3)**:** 259-274.

Wu Y, Guo L, Cui X, Chen J, Cao X and Lin H (2014), Ground-penetrating radar-based automatic reconstruction of three-dimensional coarse root system architecture, Plant and Soil, 383(1)**:** 155-172.